Available online at www.sciencedirect.com

ScienceDirect

Mendeleev Commun., 2023, **33**, 666–670

Mendeleev Communications

DFT study of the stabilization preconditions of the indoline spiropyrans with a cationic substituent

Vitaliy V. Koval,* Anastasia S. Kozlenko and Boris S. Lukyanov

Institute of Physical and Organic Chemistry, Southern Federal University, 344090 Rostov-on-Don, Russian Federation. E-mail: vitvkoval@sfedu.ru

DOI: 10.1016/j.mencom.2023.09.024

The computational modeling results are presented in the defining points of the isomerization process of the spiropyrans with cationic vinyl-3*H*-indolium substituent in the positions 6′ and 8′ of the 2*H*-chromene moiety taking into account DMSO solvent. The role of effective conjugation is revealed, that determines the significant difference in the behavior of the studied systems, based on the data of NBO energetic analysis and the atomic charge transfer analysis. The model shows that the interaction between an anion and a cation in these compounds has predominantly electrostatic nature without chemical bonds in the NBO terms.

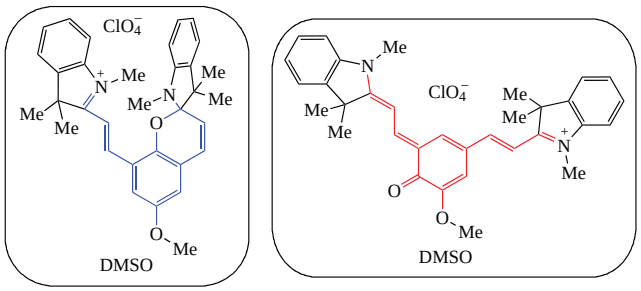

Keywords: charges, chemical bonds, density functional calculations, merocyanine, NBO theory, solvent effect, spiropyrans, indolium, chromenes.

Organic photochromic compounds of spiropyran (SPP) type can undergo reversible isomerization between closed spirocyclic (SP) and few opened merocyanine (MC) forms due to the presence of the strained C_{spiro}–O bond. Merocynines are usually active, SPPs are widely used for design of smart materials[1] and find application as sensors to the temperature and medium effects,[2,3] the presence of metals[4,5] and some anions[6,7] as well as in photobiology and photopharmacology.[8–10] The SPPs isomerization includes at least two stages: the formation of short-lived fully *cis*-MC isomer by C_{spiro}–O bond cleavage[11–13] and its further planarization into one of the more stable β-*trans*-MCs.[14–16] Until now, the reasons for this process initiation under certain conditions, and not under others, are of interest. The principal factor governing tendency of C_{spiro}–O bond to break is the electronic effects of substituents. The strongest one is the groups located in the *ortho*- and *para*-positions relative to the pyran oxygen atom. The electron-withdrawing groups (EWGs) in the *para*-position increase a lifetime of the photoinduced MC form,[17] and the presence of two EWGs[18,19] leads to the mixture of SP and MC forms in the polar solvents, even under electromagnetic radiation-free conditions. At the same time, well known spiropyran, 6′,8′-dinitro BIPS (BIPS is 1,3′,3′-trimethyl-spiro[2*H*-1-benzopyran-2,2′-indoline]), exists as a mixture of *trans-trans-cis* (TTC) and *trans-trans-trans* (TTT) MC isomers.[15] This is due to more effective distribution of the phenolate oxygen electron density and a tendency to form rather a quinonoid than a zwitterionic resonance structure.

The obtained previously compounds **1** and **2**[20] are the striking examples demonstrating the relationship between a position and a nature of a substituent and properties (Scheme 1). They contain π-electron-donating methoxy group and π-electron-withdrawing cationic 3*H*-indolium fragment in the positions 6′ and 8′ of the 2*H*-chromene moiety. It was found that there was the SP form **1a** of **1** in the DMSO solution based on the NMR data and in the solid state according to the XRD data. At the same time, for compound **2** the equilibrium mixture of SP (**2a**) and one of the MC isomers (**2c**,**d**) is formed in DMSO, but only one (**2d**) of the possible *trans*-MC forms is observed in crystals. For simple 8′-methoxy BIPS[21] and 6′-nitro-8′-methoxy BIPS[22] such behavior is not usual. The partial stabilization of the MC form can be seen as a feature of the derivative SPPs with vinyl-3*H*-indolium substituent in the position 6′, while this is unusual for 8′-cation-substituted derivatives, except the SPPs with strong EWG in the position 6′.[23] This difference in initial stability of the SP and MC forms leads to the fact that 8′-cation-substituted derivatives usually have positive photochromism while their 6′-cation-substituted ones have negative photochromism.[24,25]

The search for effective descriptors that can reliably relate the ease of cleavage of the C_{spiro}–O bond with the molecular structure has been going on for a long time. It was proposed to refer to the length and the multiplicity of the C_{spiro}–O bond, the tendency to form hydrogen bonds,[26] frontier orbitals energies and electrostatic potential distribution,[27] or a quantitative descriptor taking into account the bond length alternation along the conjugation chain.[28] Besides, the different types of atomic charges can be used to estimate the electron distribution in the molecules. However, there is no universal charge calculation scheme, which is a problem to solve. Finally, we considered the factor of DMSO to model the experimental conditions[20] and to continue the computer simulations, that began in the gas phase.[29,30] Data refinement for the gas phase[30] was made.

The calculations were performed with Gaussian 16.[31] The DFT method with the three-parameter Lee–Yang–Parr correlation functional (B3LYP)[32] and the 6-311++G(d,p) basis set[33] were used. The Polarizable Continuum Model (PCM)[34] using the integral equation formalism variant (IEFPCM)[35] was used for taking into account the solvent effect. Stationary points on the potential energy surfaces were identified by

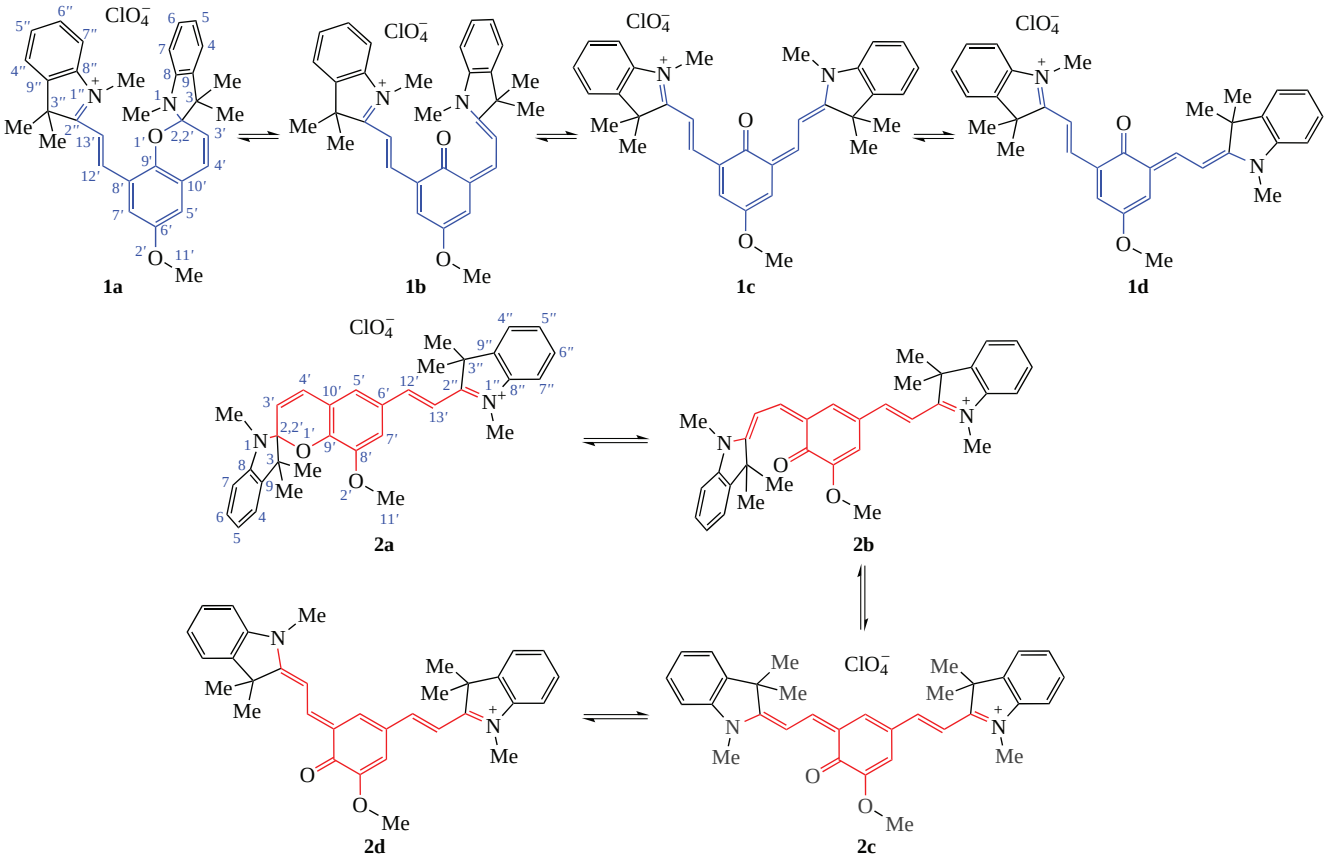

Scheme 1 Isomerization of compounds **1** and **2**. The bonds of the extended conjugation chain are colored.

calculating the matrix of force constants that were carried out analytically. To analyze the natural bond orbital (NBO), NBO 6.0 package[36] was used. The molecular structures were rendered by Chemcraft.[37]

As a starting point for the model, we used data obtained from XRD[20] for structures **1a** and **2d**. Further, we used the aforementioned process including the formation of *cis*- and *trans*-MC isomers. Its mechanism was simplified at the current stage due to the absence of possibility in the NMR experiment to examine short-lived intermediate forms[38] that are usually considered in quantum chemical computing. We suggested that in DMSO the *trans*-MC form of compound **2** could be the TTT isomer based on XRD data as well as TTC isomer based on earlier findings for similar SPPs.[15,39,40,41] Due to well-known limits of DFT calculations (for example, the computational complexity estimated as $O(N^3)$, *etc*.), the modeling approach without transition states was used. Instead, the relative positions of 3D rendered NBOs in considered structures **1a**–**d** and **2a**–**d** were manually checked. This allowed us to make sure that the modeled structures were correctly aligned with each other.

Table S2 (see Online Supplementary Materials) shows that the bond lengths of the extended conjugation chain in **1a** and **2d** have values rather close to the obtained earlier for the gas phase and XRD. There is the elongation of the double bond and the shortening of the single bonds in the carbon chains C(2,2′)–C(3′)–C(4′)–C(10′) and C(8′)–C(12′)–C(13′)–C(2″) of **1a** and **2d** in DMSO compared to the XRD data. At the same time, the conjugation becomes less pronounced than compared with gas phase calculations. Also, there are several values of the angles which noticeably differ from those obtained in both the gas phase and XRD, but this is well known property of the calculations in the different phases. Figures S1 and S2 show the role of the perchlorate anion in the geometry distortions of cation in DMSO and, for comparison, in the gas phase. This role is especially pronounced for compound **1** in the gas phase. There are lower distortions for both compounds in DMSO. In general, the geometric parameters of the built model do not contradict the data of the experiment.

The bonds between ionic fragments in the NBO terms were not found for the studied structures in DMSO as before in the gas phase.[30] So, we continue to tend to associate the interactions between anion and cation more with the electrostatic nature than with coupling between atomic orbitals, as in the gas phase.

The stabilizing effect of the localized (Lewis) and delocalized (non-Lewis) contributions in the structural stability can be estimated using the NBO energetic (deletions) analysis. There is the relation $E(\mathrm{L}) \geqslant E_{\mathrm{tot}}$, where $E(\mathrm{L})$ is the Lewis-type wavefunction energy, E_{tot} is the full energy. The value of $E(\mathrm{L})$ allows one to estimate the localized contributions, while the net energy difference $E(\mathrm{NL}) = E_{\mathrm{tot}} - E(\mathrm{L})$ allows one to estimate the delocalizing contributions. Figure 1 shows the relative values of $E(\mathrm{L})$, $E(\mathrm{NL})$ and E_{tot} for the optimized isomers of **1** and **2** in DMSO and, for comparison, in the gas phase (see Tables S3–S6 in Online Supplementary Materials).

In DMSO the stability of **1a** is favored by localized contribution, while the stability of **1b**–**d** can be attributed to the electronic delocalization energy. The difference from the gas phase is the change in the role of the localized and delocalized contributions in the structural stability of **2b**,**c**. However, the large difference in $\Delta E(\mathrm{L})$ value for **1a** and **1b** casts doubt on the possibility of further isomerization reactions regardless of DMSO factor included in the model. Also, the consideration of structures **1a**′–**d**′ without perchlorate anion shows that the pyran ring opening is not possible under normal conditions for the cation case because of the large difference in the $\Delta E(\mathrm{L})$ value for **1a**′ and **1b**′; moreover, in case DMSO this difference increases more than fourfold.

All studied isomers of **2** have corresponding $E(\mathrm{L})$ and $E(\mathrm{NL})$ values of similar order in DMSO as in the gas phase. Thus, from the point of view of the balance between the $E(\mathrm{L})$ and $E(\mathrm{NL})$

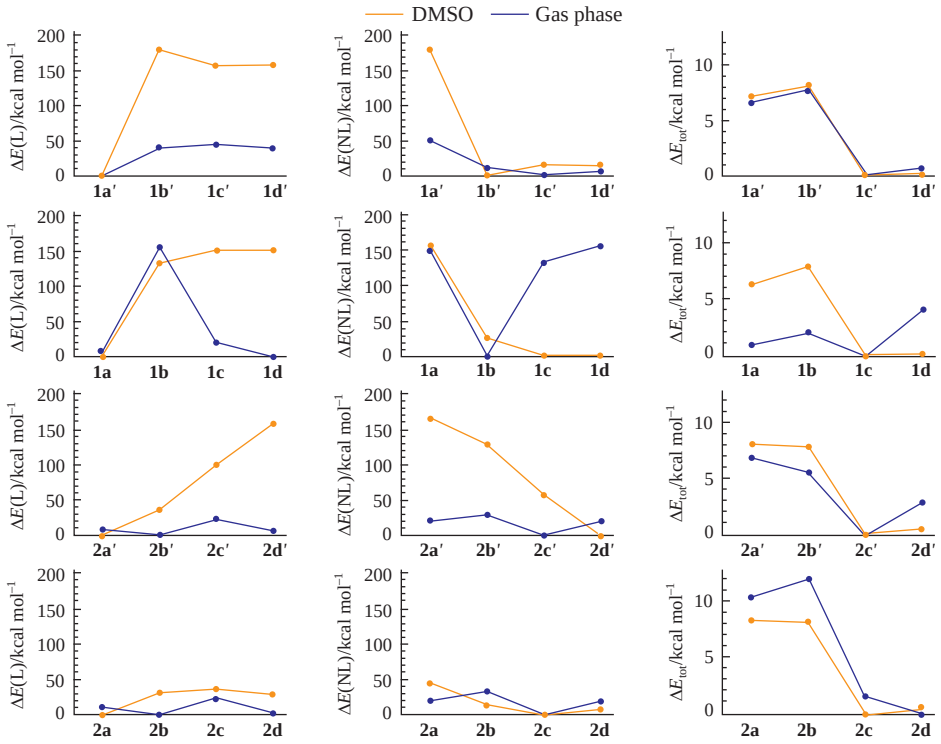

Figure 1 Diagrams of the Lewis-type wavefunction energy E(L), the net energy difference E(NL) and the total electronic energy E_{tot} for isomeric structures with perchlorate anion (**1a**–**d**, **2a**–**d**) and without it (**1a′**–**d′**, **2a′**–**d′**) in DMSO and in the gas phase.

contributions, all structures **2a**–**d** are possible whereas **2a** has become more preferable than **2b** due to the ΔE(L) value equal to 30.6 kcal mol^{-1} (in the gas phase the situation is reversed and ΔE(L) = 10.3 kcal mol^{-1}). Also, there is ΔE(NL) > 2.5 ΔE(L) for **2b** and **2c** (ΔE(NL) > 1.4 ΔE(L) according to updated data for the gas phase). This may point to the stabilizing factors other than the expected steric and electrostatic ones. Without perchlorate anion, **2c′** is more preferable than **2d′** due to the E(L) contribution, and this isomerization becomes impossible, that is different from the situation in the gas phase. This indicates the pronounced effects of the anion and the solvent on the molecular properties in the considered case.

So, the balance between the E(L) and E(NL) contributions affects the C_{spiro}–O bond preservation for **1** and its breaking and further stabilization of MC forms for **2** in DMSO, which is consistent with updated data for the gas phase.

In transitions from **1a** consistently to **1d** the energy changes ΔE_{tot} lie within 0.2–7.9 kcal mol^{-1} for DMSO and 1.1–4.2 kcal mol^{-1} for the gas phase. However, since the thermodynamic barriers of isomerization reactions are unknown at this stage of the research, further the studied process was considered not from physical-chemical, but from chemical-physical point of view. In addition to the NBO energetic analysis, we investigated the process of atomic charge transfer (CT), occurring during isomerization along the extended conjugation chains (see Scheme 1). In order to select the most appropriate method to describe this process, the Mulliken (MPA) charges, the atomic polar tensor (APT) charges, the electrostatic potential population (ESP) charges and the natural population analysis (NPA) charges were considered. The MPA, APT and ESP calculations schemas were examined with and without hydrogens summed into heavy atoms. It was found that any of the listed schemas can be used to describe the simulated process, because each of them allows us to identify the main regularities of the studied process with the technical absence of experimental data for atomic charges in our compounds.

Figure 2 illustrates the method to describe CT along the extended conjugation chains at the endpoints of the process of the pyran ring opening in **1** and **2**, that made using MPA charges histograms. In Figures S3–S6 (see Online Supplementary Materials), there are all histograms used to study CT during the transitions between **1a**–**d** and **2a**–**d**. Histograms are based on values from Table S7 and they are primarily designed to determine the quality features of studied process. In Tables S8–S10, there are the statistical data obtained during processing the values of Table S7. This allows the process to be quantified as far as possible.

According to any of examined calculation schemas, the charge change of thousands of percent is required on atoms of

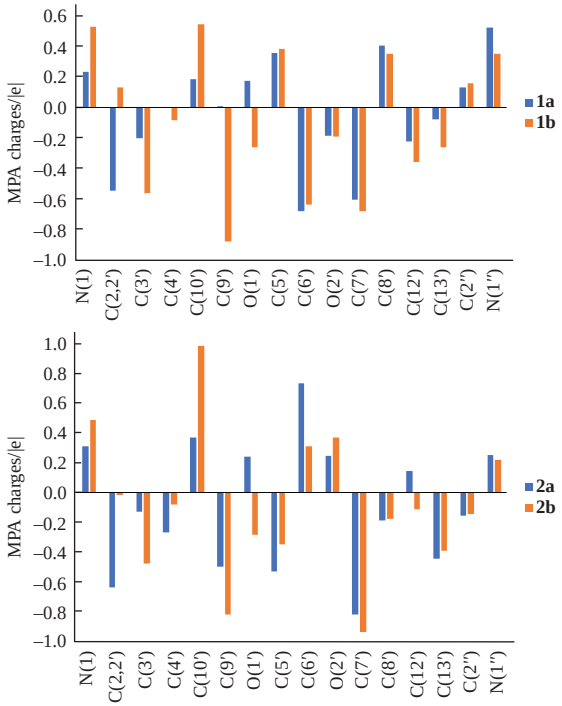

Figure 2 Histograms of the MPA charges for isomeric structures **1a**,**b** and **2a**,**b**, corresponding to the endpoints of process of the pyran ring opening in **1** and **2**, respectively.

the pyran ring during its opening in compound **1**, while in compound **2** this is only hundreds of percent. The NPA schema is an exception due to its definition, but it can be used in combination with the results of the NBO energetic analysis. For example, large changes in atomic charges during transition from **2a** to **2b** correspond to delocalized contributions in the structural stability of **2b** (see Figures 1, S3 and Tables S7, S8).

At the same time, the pyran ring opening is accompanied by CT along all chain between nitrogen atoms of the indoline ring and the indolium cycle. The value of CT for **1** is greater than that one for **2**. This leads to the conclusion about the role of effective conjugation in the isomerization reactions, determined by the structure of studied compounds.

It should be noted that during examination of further isomerization stages, the charges of C(5′), C(6′) and C(7′), C(8′) of structure **1** should be correspondingly compared with the charges of C(7′), C(8′) and C(5′), C(6′) of **2**, based on the position of the vinyl-3*H*-indolium substituent and methoxy group in the molecule. Also, the hydrogens, summed into heavy atoms, have a noticeable effect in several cases, but they do not change the general picture.

The transitions from the *cis*-MC **1b** and **2b** to the corresponding TTC-TTC *trans*-MC **1c** and **2c** is accompanied by CT comparable with one found during the transition from **2a** to **2b**. That is, the charge changes permit both transitions. Charge transfer may concentrate near any of the nitrogen-containing cycles depending on the calculation schema used, but this is acceptable for describing the studied processes under current technical limits. The transition from **2c** to **2d** is accompanied by CT with the values comparable to those found during the transition from **2a** to **2b**. For the transition from **1c** to **1d** such values are several times greater. So, the hypothetical transition from **1c** to **1d** requires rather large CT. For compound **2** such transition is not limited by the CT values. This should be the topic of further investigations.

To conclude, it is possible to say that the necessity of a significant CT can lead to the pyran ring preservation in compound **1**, that, in turn, is due to the more pronounced localization of the electron density in different parts of the molecule. The latter can be associated with a less pronounced conjugation effect. The model of compounds **1**, **2** investigated in DMSO was created by a constructive method of computational experiment. The qualitative behavior of the model is reasonably consistent with existing observations in the natural experiment based on NMR and XRD data as well as with earlier calculations in the gas phase. The data of localized and delocalized contributions to structural stability and data of CT were obtained in the defining points of the isomerization process taking into account the DMSO factor. These data explain the difference in observed behavior of the investigated compounds and open opportunities for further study. The results of NBO analysis of the studied compounds lead to the conclusion about the electrostatic nature of the interaction between an anion and a cation in the absence of chemical bonds in the NBO terms.

This research was financially supported by the Ministry of Science and Higher Education of the Russian Federation (State assignment in the field of scientific activity, grant no. FENW-2023-0020).

Online Supplementary Materials

Supplementary data associated with this article can be found in the online version at doi: 10.1016/j.mencom.2023.09.024.

References

1 R. Klajn, *Chem. Soc. Rev.*, 2014, **43**, 148.
2 M. Gao, C. Lian, R. Xing, J. Wang, X. Wang and Z. Tian, *New J. Chem.*, 2020, **44**, 15350.
3 Y. Shiraishi, M. Itoh and T. Hirai, *Phys. Chem. Chem. Phys.*, 2010, **12**, 13737.
4 J. Kang, E. Li, L. Cui, Q. Shao, C. Yin and F. Cheng, *Sens. Actuators, B*, 2021, **327**, 128941.
5 A. V. Chernyshev, A. V. Metelitsa, I. A. Rostovtseva, N. A. Voloshin, E. V. Solov'eva, E. B. Gaeva and V. I. Minkin, *J. Photochem. Photobiol., A*, 2018, **360**, 174.
6 K. Prakash, P. R. Sahoo and S. Kumar, *Sens. Actuators, B*, 2016, **237**, 856.
7 S. Samanta, S. Halder, U. Manna and G. Das, *J. Chem. Sci.*, 2019, **131**, 36.
8 F. Cardano, E. Del Cantoc and S. Giordani, *Dalton Trans.*, 2019, **48**, 15537.
9 S. Barman, J. Das, S. Biswas, T. K. Maitib and N. D. Pradeep Singh, *J. Mater. Chem. B*, 2017, **5**, 3940.
10 W. A. Velema, M. J. Hansen, M. M. Lerch, A. J. M. Driessen, W. Szymanski and B. L. Feringa, *Bioconjugate Chem.*, 2015, **26**, 2592.
11 R. A. Rogers, A. R. Rodier, J. A. Stanley, N. A. Douglas, X. Li and W. J. Brittain, *Chem. Commun.*, 2014, **50**, 3424.
12 P. Naumov, P. Yu and K. Sakurai, *J. Phys. Chem. A*, 2008, **112**, 5810.
13 V. I. Minkin, A. V. Metelitsa, I. V. Dorogan, B. S. Lukyanov, S. O. Besugliy and J.-C. Micheau, *J. Phys. Chem. A*, 2005, **109**, 9605.
14 C. B. Aakeröy, E. P. Hurley, J. Desper, M. Natali, A. Douglawib and S. Giordani, *CrystEngComm*, 2010, **12**, 1027.
15 J. Hobley, V. Malatesta, R. Millini, L. Montanari and W. O'Neil Parker, Jr., *Phys. Chem. Chem. Phys.*, 1999, **1**, 3259.
16 P. Nuernberger, S. Ruetzel and T. Brixner, *Angew. Chem., Int. Ed.*, 2015, **54**, 11368.
17 E. I. Balmond, B. K. Tautges, A. L. Faulkner, V. W. Or, B. M. Hodur, J. T. Shaw and A. Y. Louie, *J. Org. Chem.*, 2016, **81**, 8744.
18 S. Toppet, W. Quintens and G. Smets, *Tetrahedron*, 1975, **31**, 1957.
19 M. Schulz-Senft, P. J. Gates, F. D. Sönnichsen and A. Staubitz, *Dyes Pigm.*, 2017, **136**, 292.
20 M. B. Lukyanova, V. V. Tkachev, B. S. Lukyanov, A. D. Pugachev, I. V. Ozhogin, O. A. Komissarova, S. M. Aldoshin and V. I. Minkin, *J. Struct. Chem.*, 2018, **59**, 565.
21 S. K. Rastogi, Z. Zhao, M. B. Gildner, B. A. Shoulders, T. L. Velasquez, M. O. Blumenthal, L. Wang, X. Li, T. W. Hudnall, T. Betancourt, L. Du and W. J. Brittain, *Tetrahedron*, 2021, **80**, 131854.
22 T. J. Feuerstein, R. Müller, C. Barner-Kowollik and P. W. Roesky, *Inorg. Chem.*, 2019, **58**, 15479.
23 A. S. Kozlenko, N. I. Makarova, I. V. Ozhogin, A. D. Pugachev, M. B. Lukyanova, I. A. Rostovtseva, G. S. Borodkin, N. V. Stankevich, A. V. Metelitsa and B. S. Lukyanov, *Mendeleev Commun.*, 2021, **31**, 403.
24 A. D. Pugachev, I. V. Ozhogin, M. B. Lukyanova, B. S. Lukyanov, A. S. Kozlenko, I. A. Rostovtseva, N. I. Makarova, V. V. Tkachev, S. M. Aldoshin and A. V. Metelitsa, *J. Mol. Struct.*, 2021, **1229**, 129615.
25 A. D. Pugachev, I. V. Ozhogin, N. I. Makarova, I. A. Rostovtseva, M. B. Lukyanova, A. S. Kozlenko, G. S. Borodkin, V. V. Tkachev, I. M. El-Sewify, I. V. Dorogan, A. V. Metelitsa, S. M. Aldoshin and B. S. Lukyanov, *Dyes Pigm.*, 2022, **199**, 110043.
26 S. M. Aldoshin, *Russ. Chem. Rev.*, 1990, **59**, 663 (*Usp. Khim.*, 1990, **59**, 1144).
27 M. S. A. Abdel-Mottaleb and S. N. Ali, *Int. J. Photoenergy*, 2016, 6765805.
28 P.-X. Wang, F.-Q. Bai, Z.-X. Zhang, Y.-P. Wang, J. Wang and H.-X. Zhang, *Org. Electron.*, 2017, **45**, 33.
29 V. V. Koval, A. S. Kozlenko, V. I. Minkin and B. S. Lukyanov, *Russ. J. Gen. Chem.*, 2021, **91**, 1150 (*Zh. Obshch. Khim.*, 2021, **91**, 977).
30 V. V. Koval, A. S. Kozlenko, V. I. Minkin, I. M. El-Sewify and B. S. Lukyanov, *Mendeleev Commun.*, 2022, **32**, 467.
31 M. J. Frisch, G. W. Trucks, H. B. Schlegel, F. Lipparini, F. Egidi, J. Goings, B. Peng, A. Petrone, T. Henderson, D. Ranasinghe, V. G. Zakrzewski, J. Gao, N. Rega, G. Zheng, W. Liang, M. Hada, M. Ehara, K. Toyota, R. Fukuda, J. Hasegawa, M. Ishida, T. Nakajima, Y. Honda, O. Kitao, H. Nakai, T. Vreven, K. Throssell, J. A. Montgomery Jr., J. E. Peralta, F. Ogliaro, M. J. Bearpark, J. J. Heyd, E. N. Brothers, K. N. Kudin, V. N. Staroverov, T. A. Keith, R. Kobayashi, J. Normand, K. Raghavachari, A. P. Rendell, J. C. Burant, S. S. Iyengar, J. Tomasi, M. Cossi, J. M. Millam, M. Klene, C. Adamo, R. Cammi, J. W. Ochterski, R. L. Martin, K. Morokuma, O. Farkas, J. B. Foresman and D. J. Fox, *Gaussian 16, Revision C.01*, Gaussian, Wallingford, CT, 2016.
32 A. D. Becke, *J. Chem. Phys.*, 1993, **98**, 5648.
33 R. Krishnan, J. S. Binkley, R. Seeger and J. A. Pople, *J. Chem. Phys.* 1980, **72**, 650.
34 J. Tomasi, B. Mennucci and R. Cammi, *Chem. Rev.*, 2005, **105**, 2999.
35 E. Cancès, B. Mennucci and J. Tomasi, *J. Chem. Phys.*, 1997, **107**, 3032.

36 E. D. Glendening, J. K. Badenhoop, A. E. Reed, J. E. Carpenter, J. A. Bohmann, C. M. Morales, C. R. Landis and F. Weinhold, *NBO 6.0*, Theoretical Chemistry Institute, University of Wisconsin, Madison, WI, 2013.
37 G. A. Zhurko, *Chemcraft – Graphical Program for Visualization of Quantum Chemistry Computations*, Ivanovo, Russia, 2005, https://chemcraftprog.com.
38 I. V. Dorogan and V. I. Minkin, *Chem. Heterocycl. Compd*., 2016, **52**, 730.
39 J. Hobley and V. Malatesta, *Phys. Chem. Chem. Phys.*, 2000, **2**, 57.
40 G. Cottone, R. Noto and G. La Manna, *Chem. Phys. Lett.*, 2004, **388**, 218.
41 A. Metelitsa, A. Chernyshev, N. Voloshin, E. Solov'eva, I. Rostovtseva, I. Dorogan, E. Gaeva and A. Guseva, *Dyes Pigm.*, 2021, **186**, 109070.

Received: 25th April 2023; Com. 23/7156